Neutron Diffraction Study of Manganese Ferrite*

Julius M. Hastings and Lester M. Corliss
Department of Chemistry, Brookhaven National Laboratory, Upton, New York
(Received July 6, 1956)

Neutron diffraction patterns have been obtained for polycrystalline $MnFe_2O_4$ at 300°K and 4.2°K. The fraction of tetrahedral sites occupied by Mn^{+2} has been found to be 0.81±0.03, indicating that $MnFe_2O_4$ has very nearly the normal spinel structure. The value 0.3846±0.0003 has been assigned to the space group parameter u. The observed magnetic scattering is consistent with the Néel model and with the measured saturation moment.

INTRODUCTION

THE distribution of metal ions between tetrahedral and octahedral sites in $MnFe_2O_4$ has long been of interest in connection with the general understanding of magnetic interactions in spinels and more particularly in connection with the Néel theory of ferrimagnetism.[1,2] Since Mn^{+2} and Fe^{+3} have the same electronic configurations it is impossible, on the basis of saturation magnetization measurements, to choose between alternative distributions. X-ray diffraction techniques are likewise incapable of satisfactorily distinguishing between these two species and hence are unsuited to a determination of the cation distribution.

Verwey and Heilmann[3] have examined the unit cell dimensions of spinels having the general formula XY_2O_4 where X represents divalent Ni, Cu, Zn, Mg, Co, Fe, Mn, Cd, and Y represents trivalent Cr and Fe. They point out that the lattice parameter, a_0, increases by an amount equal to 0.04 to 0.06 A in going from the Cr^{+3} spinel structure to the Fe^{+3} spinel structure, except in the case of Zn^{+2} and Cd^{+2} which are known from x-ray data to be normal spinels and for which the increase in a_0 is 0.12 A. Since $CuFe_2O_4$ and $MgFe_2O_4$

were known at the time to be substantially inverted, the authors concluded that $MnFe_2O_4$ as well as the ferrites of Fe^{+2}, Co^{+2}, and Ni^{+2} were probably also inverted.

From the point of view of the determination of the ionic distribution, $MnFe_2O_4$ constitutes a particularly favorable case for neutron diffraction. The nuclear scattering amplitudes of Mn and Fe differ in magnitude, by a factor of about 2.5 and possess, in addition, opposite signs. The sensitivity of the effective scattering amplitudes of the two kinds of crystallographic sites to changes in population is thus greatly enhanced. In addition to the "chemical" information provided by the neutron diffraction pattern, the coherent magnetic scattering arising from the alignment of electronic magnetic moments determines the average moment to be associated with each kind of crystallographic site. The magnitude and relative orientation of the individual moments can be compared directly with the predictions of the Néel theory.

EXPERIMENTAL

Three separate preparations of $MnFe_2O_4$ listed in Table I were examined during the course of this investigation. Despite the very different firing conditions, only minor quantitative variations were observed in the neutron diffraction patterns. Hence, all the following discussion will be restricted to sample C unless otherwise noted. An analysis by Dr. R. W. Stoenner of Brookhaven National Laboratory showed 23.36 percent
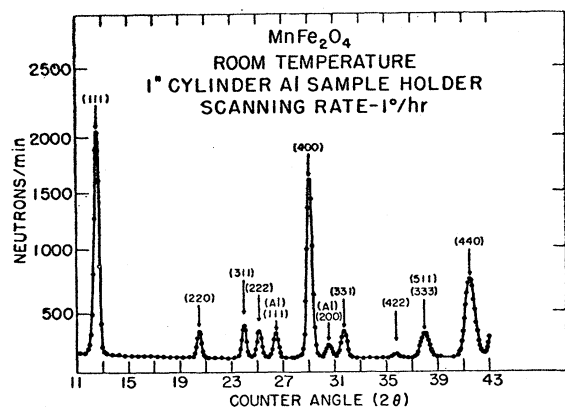

Fig. 1. Neutron diffraction pattern of $MnFe_2O_4$ at room temperature.

[1] L. Néel, Ann. phys. 3, 139 (1948).
[2] E. W. Gorter, Philips Research Repts. 9, 295–365, 403–443 (1954), thesis, University of Leyden, June, 1954.
[3] E. J. W. Verwey and E. L. Heilmann, J. Chem. Phys. 15, 174 (1947).
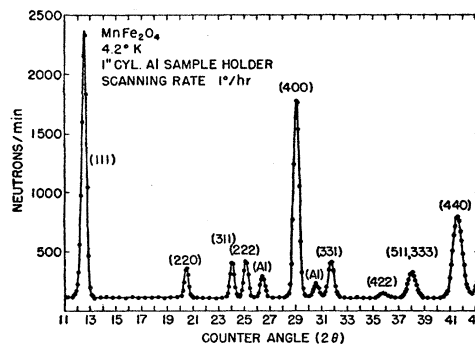

Fig. 2. Neutron diffraction pattern of $MnFe_2O_4$ at liquid helium temperature.

TABLE I. Data summary for various preparations of manganese ferrite.

Sample	Source	Firing conditions	μ_β (4.2°K)	x Fraction of A sites occupied by Mn^{+2}	u oxygen space group parameter
A	Dr. V. C. Wilson G. E. Research Laboratory	4 hours–1200°C N₂ atmosphere	4.6	0.79	0.385
B	Dr. L. G. van Uitert Bell Telephone Laboratories	6 hours–1300°C 2000 ml/min N₂ 5 ml/min O₂ slow cooling in N₂	4.6	0.82	0.386
C	Dr. C. J. Kriessman Remington-Rand	24 hours–1400°C air atmosphere water quench	4.60	0.81	0.384₆

manganese and 48.65% iron compared with the stoichiometric composition of 23.82% manganese and 48.44% iron. The saturation magnetization was measured at 300°K, 77°K, and 4.2°K using a ballistic method and values of 3.27, 4.47, and 4.60 Bohr magnetons respectively were obtained. The unit cell edge, a_0, was found to be 8.517 angstroms for this preparation.

All the neutron diffraction patterns were made on 325 mesh powders using a wavelength of 1.064 A. The high angle measurements, using sample A, were made on a flat glass-walled cell of dimensions $\frac{1}{2} \times 2\frac{1}{2} \times 4$ inches. All the other data were obtained using a double-jacketed vacuum cryostat similar to that described by Erickson.[4] The samples were contained in an aluminum cylinder, $2\frac{1}{2}$ inches long and 1 inch inside diameter. The patterns are shown in Figs. 1, 2, and 3.

Method of Analysis

A complete interpretation of the neutron diffraction pattern of MnFe₂O₄ involves a determination of both the "chemical" and "magnetic" structures. The chemical structure gives rise to the purely nuclear scattering part of the diffraction pattern and is characterized by two parameters, x and u. The x parameter gives the fraction of tetrahedral or A sites occupied by Mn^{+2} and hence describes the metal ion distribution. The other parameter, u, fixes the oxygen positions in the spinel structure and a deviation from the value 0.375 implies a distortion from cubic close packing of the oxygen ions. The magnetic structure gives rise to additional scattering which is superimposed on the nuclear scattering. This additional scattering depends on the magnetic moments to be associated with individual lattice sites, their orientation relative to each other and also on the magnetic form factor.

Several methods are available for separating the magnetic and nuclear contributions to the diffraction peaks. Application of an external magnetic field directed parallel to the scattering vector removes the magnetic

component provided the field is uniform and sufficiently high to saturate the sample in the desired direction. A second procedure is to raise the temperature of the sample above the magnetic Curie point. This is useful for inert materials or where provision can be made to prevent chemical change. In the present instance it was found most convenient to isolate the nuclear contribution by making use of diffraction data taken at high angles where the magnetic contributions are sufficiently diminished by the form factor dependence of the magnetic scattering amplitude. At a value of $4\pi(\sin\theta)/\lambda$ equal to 5, for example, the square of the magnetic structure factor has already decreased to about 10 percent of its value for the forward direction. The high angle diffraction pattern shown in Fig. 3 is produced almost entirely by the nuclear scattering. Intensities and resolution are sufficiently good to provide useful qualitative information for the analysis.

Preliminary values for the structural parameters, x and u, were obtained by trial and error calculations, using the outer peak intensities. With these values the nuclear contributions to the inner peaks were calculated. The magnetic scattering intensities, obtained by sub-
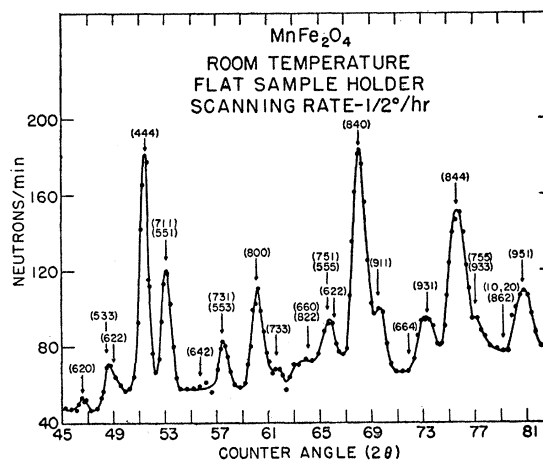

FIG. 3. High angle neutron diffraction pattern of MnFe₂O₄ with improved resolution.
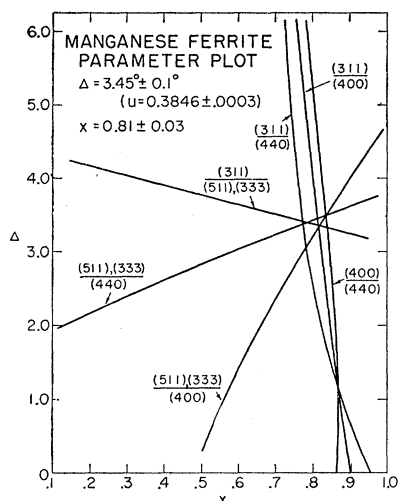
[4] R. A. Erickson, Phys. Rev. 90, 779 (1953).

FIG. 4. Graphical determination of u and x parameters characterizing chemical structure.

TABLE II. Comparison of calculated and observed intensities for MnFe$_2$O$_4$.

hkl	$I_{nuc.}$ (calc)	300°K ($\mu = 3.23$)			4.2°K ($\mu = 4.60$)		
		$I_{mag.}$ (calc)	$I_{tot.}$ (calc)	I_{obs}	$I_{mag.}$ (calc)	$I_{tot.}$ (calc)	I_{obs}
111	714	871	1585	1620	1144	1858	1990
220	2	150	152	158	164	166	169
311	217	4	221	231	17	234	240
222	53	155	208	199	230	283	258
400	1362	182	1544	1520	245	1607	1640
331	94	179	273	257	236	330	328
422	5	47	52	40	52	57	56
511,333	312	1	313	343	5	317	316
440	1240	7	1247	1270	15	1255	1240

$$\Delta\frac{calc}{obs} = 3.5\% \qquad \Delta\frac{calc}{obs} = 2.7\%$$

traction of the calculated approximate nuclear contributions, agreed qualitatively with those computed from the Néel model and the observed moment. In addition, the (311), (400), (511), (333), and (440) peaks were found to be almost entirely nuclear in origin. These intensities were corrected for small magnetic contaminations by applying the Néel model and were then used for a final refinement of the structural parameters, x and u. This determination was made graphically by first constructing plots of calculated intensity ratios as a function of the degree of inversion, x, for various values of the oxygen parameter, u. The observed ratio for a given pair of reflections was then entered on the plot for the corresponding calculated ratio as a horizontal line. The intersections of this line with the curves computed for the given peak ratio and various values of the u parameter determine u as a function of the degree of inversion. This procedure results in a series of u vs x curves each consistent with an individual experimental intensity ratio, as shown in Fig. 4, where the ordinate is given in terms of the more sensitive angular parameter, $\Delta° = 360°u - 135°$. The curves have a common intersection simultaneously satisfying all the intensity requirements at $x = 0.81 \pm 0.03$ and $\Delta = 3.45° \pm 0.1°$ (or $u = 0.3846 \pm 0.0003$).

Table I presents a summary of the results obtained for all three preparations of manganese ferrite. The values for the fraction of tetrahedral sites occupied by manganese are seen to cluster around 0.80, indicating that manganese ferrite is more nearly normal than inverted.

The coherent magnetic contribution to the diffraction pattern was obtained by subtracting the computed nuclear part from the observed pattern. The first six magnetic peak intensities thus obtained were fitted by adjusting two parameters; namely, the average magnetic scattering amplitudes for octahedral and for tetrahedral sites. The macroscopic saturation moment can be computed from these individual moments according to the formula $\mu = 2\mu_B + \mu_A$, in which μ_A and μ_B have opposite signs. In the case of sample C of Table I, for which extensive measurements were made, the saturation moments deduced from the diffraction data were $3.23\mu_\beta \pm 0.3$ and $4.60\mu_\beta \pm 0.2$ at 300°K and 4.2°K, respectively. These compare very favorably with the corresponding values obtained by magnetic measurements on the same sample of $3.27\mu_\beta$ (300°K) and $4.60\mu_\beta$ (4.2°K). The individual moments for A and B sites at 300°K were $|\mu_A| = 4.33\mu_\beta$ and $|\mu_B| = 3.78\mu_\beta$, while at 4.2°K the values $|\mu_A| = |\mu_B| = 4.60\mu_\beta$ were obtained. There is thus an indication that the A and B sites are saturated to different extents at room temperature. The moments on A and B sites were found to be oppositely directed, as expected from the Néel model.

The over-all agreement between observed and calculated intensities for sample C is shown in Table II and is seen to be quite satisfactory. The magnetic contributions were calculated using the zinc ferrite form factor.[5] The internal consistency obtained in this way was somewhat better than that which could be gotten using the form factor previously deduced for nickel ferrite and magnesium ferrite.[6] This may be related to the fact that manganese ferrite is more nearly normal than inverted. In computing the nuclear contributions, the oxygen parameter and the degree of inversion were taken to be the same at both 300°K and 4.2°K.

DISCUSSION

The saturation moment of MnFe$_2$O$_4$ has been measured by several workers, all but one of whom report values below $5\mu_\beta$ per molecule.[2] Since both Mn^{+2} and Fe^{+3} are in S states with spin 5/2, the Néel model would predict a value of $5\mu_\beta$ independent of the cation distribution. Various explanations have been offered to

[5] Brockhouse, Corliss, and Hastings, Phys. Rev. 98, 1721 (1955).
[6] Corliss, Hastings, and Brockman, Phys. Rev. 90, 1013 (1953).

account for this anomaly and it was hoped, at the outset, that the neutron diffraction results might decide which of these was correct. There are, however, a number of uncertainties which limit the accuracy of the method and rule out the possibility of a precise measurement of the individual moments of the ions on A and B sites. As has been noted, the nuclear and magnetic Bragg reflections are superimposed. Thus, any errors in the determination of the parameters which fix the chemical unit cell are reflected in the magnetic scattering pattern, which is obtained by difference. Furthermore, the magnetic scattering has a form factor dependence which cannot be determined independently and must therefore be treated as a parameter in the analysis. In addition there are uncertainties in the stoichiometry. An over-all estimate of these errors rules out the possibility of deciding any

subtle questions such as partial oxidation-reduction of Mn^{+2}-Fe^{+3} which would account for the anomalous moment.

SUMMARY

The neutron diffraction data are in good agreement with the Néel model of ferrimagnetism. The large difference in the coherent scattering amplitudes of iron and manganese enables one to fix the cation distribution rather precisely. The observed magnetic scattering is consistent with the measured saturation magnetization at both room temperature and liquid helium temperature.

ACKNOWLEDGMENTS

Scattering of Holes by Phonons in Germanium*

H. Ehrenreich,† *General Electric Research Laboratory, Schenectady, New York*

AND

A. W. Overhauser, *Department of Physics, Cornell University, Ithaca, New York*
(Received March 28, 1956)

The lattice scattering of holes within and between the two valence bands of germanium, degenerate at $k=0$, is calculated. Scattering by both acoustical and optical modes is considered. The electron-lattice interaction Hamiltonian is seen to be separable into two parts: the first, associated with acoustical modes, arises from vibrations of the unit cells as a whole and the other, associated with both acoustical and optical modes, arises from the relative motion of the two atoms in the unit cell of the germanium lattice. The matrix elements for scattering are expressible in terms of two constants, C_1 and C_4, associated respectively with the two parts of the interaction Hamiltonian. The wave functions used to calculate the matrix elements are determined by $k \cdot p$ and spin-orbit perturbations and assume spherical surfaces of constant energy in k-space and a parabolic relation between energy and wave number. For the terms in C_1 the scattering is treated using both the deformable and rigid ion models. The angular distributions for scattering are such that heavy holes are scattered predominantly in the forward direction and light holes in the backward direction for the deformable ion model, whereas the opposite is true for the rigid ion model. The scattering resulting from transverse and longitudinal phonons is about equally important for deformable ions; for rigid ions scattering by transverse modes is less significant. The matrix elements depending on C_4 are obtained from the rigid ion model alone. The transition probabilities for scattering are presented in a form which can be applied readily to the transport properties of germanium.

1. INTRODUCTION

THE temperature dependence of the lattice scattering mobility of holes in germanium has been determined experimentally[1] as about $T^{-2.3}$, in a range of temperatures, extending roughly between 100°K and

300°K, for which the lattice vibrations are the dominant mechanism for scattering. This result is in disagreement with the theoretically predicted temperature dependence of $T^{-1.5}$, obtained by assuming that conduction takes place in a single valence band whose wave functions and energy surfaces near the band edge, at $k=0$, have spherical symmetry.[2]

Because of this disagreement, it is necessary to reconsider the problem of the lattice-scattering mobility of holes in the light of the information concerning the valence band structure that is now available. The

[1] F. J. Morin, Phys. Rev. **93**, 62 (1953); M. B. Prince, Phys. Rev. **92**, 681 (1953); F. J. Morin and J. P. Maita, Phys. Rev. **94**, 1525 (1954).

[2] F. Seitz, Phys. Rev. **73**, 549 (1948); J. Bardeen and W. Shockley, Phys. Rev. **80**, 72 (1950).